



Citation for published version:

Dodwell, TJ, Butler, R & Rhead, AT 2016, 'Optimum fibre-steering of composite plates for buckling and manufacturability', *AIAA Journal*, vol. 54, no. 3, pp. 1139-1142. <https://doi.org/10.2514/1.J054297>

DOI:

[10.2514/1.J054297](https://doi.org/10.2514/1.J054297)

Publication date:

2016

Document Version

Early version, also known as pre-print

[Link to publication](#)

University of Bath

Alternative formats

If you require this document in an alternative format, please contact:
openaccess@bath.ac.uk

General rights

Copyright and moral rights for the publications made accessible in the public portal are retained by the authors and/or other copyright owners and it is a condition of accessing publications that users recognise and abide by the legal requirements associated with these rights.

Take down policy

If you believe that this document breaches copyright please contact us providing details, and we will remove access to the work immediately and investigate your claim.

See discussions, stats, and author profiles for this publication at: <http://www.researchgate.net/publication/271748228>

Optimum Fibre-Steering of Composite Plates for Buckling and Manufacturability

ARTICLE in AIAA JOURNAL · OCTOBER 2015

Impact Factor: 1.21

READS

86

3 AUTHORS, INCLUDING:



Timothy James Dodwell

University of Exeter

26 PUBLICATIONS 64 CITATIONS

SEE PROFILE



Andrew Rhead

University of Bath

13 PUBLICATIONS 55 CITATIONS

SEE PROFILE

Optimum Fiber-Steering of Composite Plates for Buckling and Manufacturability

Timothy J. Dodwell*, Richard Butler† and Andrew T. Rhead‡

College of Mathematics, Engineering and Physical Sciences, University of Exeter, Exeter, EX4 4PY.

Department of Mechanical Engineering, University of Bath, Bath, BA2 7AY.

Nomenclature

P_x^c	critical buckling load, kN
$\kappa(\theta)$	curvature of tow path, mm^{-1}
ρ	density, kgmm^{-3}
E_{ij}	direct in-plane elastic moduli, kNmm^{-2}
θ	fibre angle, degrees
P_x	in-plane load, kN
N	number of control points
ν_{ij}	in-plane Poisson's ratios
G_{ij}	in-plane shear moduli, kNmm^{-2}
A, D and H	laminate stiffness matrices for in-plane, out-of-plane and through-thickness shear, kNmm^{-2}
L_x, L_y	length and width of panel, mm
M	mass, kg
N_{ply}	Number of plies
R	radius of curvature, mm
$t_b, t(\theta)$	un-sheared and variable ply thickness, mm
T	laminate thickness, mm
w_i	width of strip, mm

*Lecturer, College of Mathematics, Engineering and Physical Sciences, Email: t.dodwell@exeter.ac.uk

†Professor, Department of Mechanical Engineering, Email: r.butler@bath.ac.uk

‡Lecturer, Department of Mechanical Engineering, Email: a.t.rhead@bath.ac.uk

ℓ width of tow, mm

Subscript

i, j either local direction parameters or dummy indices

x, y global direction parameters

I. Introduction

The basic advantages of carbon fiber reinforced plastics (CFRP) are well established. In aerospace, and other applications where both efficiency and safety are paramount, fibers are orientated to maximise structural efficiency. Typically, laminates comprise of plies with one of four straight fiber orientations ($0^\circ, \pm 45^\circ, 90^\circ$). Recently, variable angle tow (VAT) composites, in which fiber orientation varies within a layer have attracted significant attention. VAT designs have been used to tailor in-plane stiffness for improved buckling and post-buckling performance of plates^{1,2} and cylindrical shells,³ whilst significant stress relief can be achieved around cut-outs.⁴ Automated Fiber Placement (AFP) technology is widely used in industry to

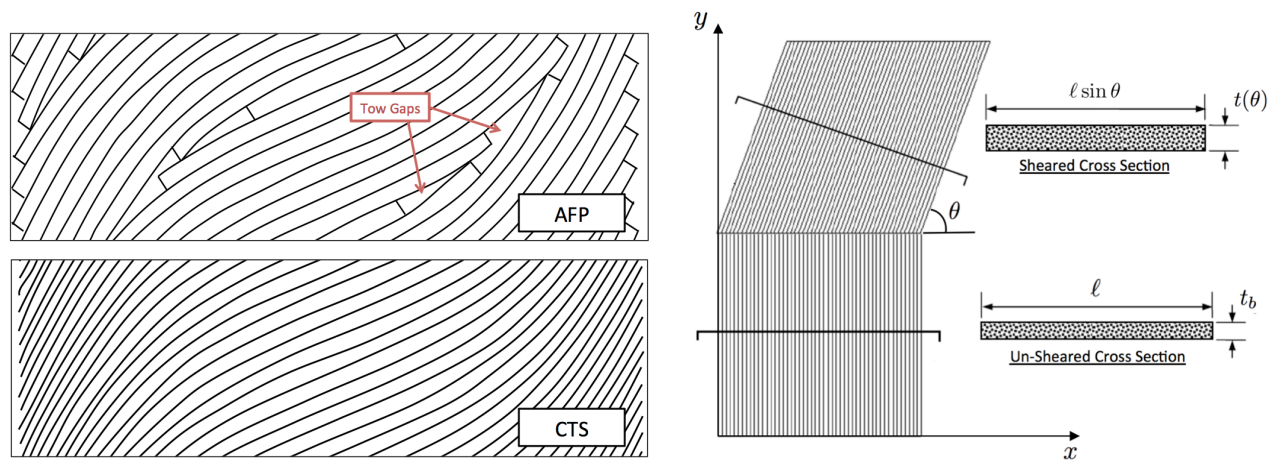


Figure 1: (Left) Non-tessellating AFP and tessellating CTS tow courses. (Right) Demonstrates the connection between shearing angle θ and ply thickness t in the CTS process.

lay tows of CFRP and has the capability to deliver curved fiber paths. However, the AFP head is constrained to remain perpendicular to the fiber course, and curvature is achieved by bending the material in-plane. For radii of curvatures $< 500\text{mm}$, 1/4 inch tows are increasingly susceptible to manufacturing defects such as wrinkling⁵ [6, Sec 5.], tow gaps and overlaps.⁷ A new technology, Continuous Tow Shearing (CTS), changes fiber orientation dynamically by shearing dry fibers in-plane, after which resin is impregnated by the machine head 'on-the-fly'.⁸ CTS opens up the design space of manufacturable fiber paths by permitting tow radii as small as 30mm whilst maintaining the fiber tow tessellation required for defect-free panels, Fig. 1. Furthermore, CTS can be used to manipulate local thicknesses. This additional degree of freedom arises

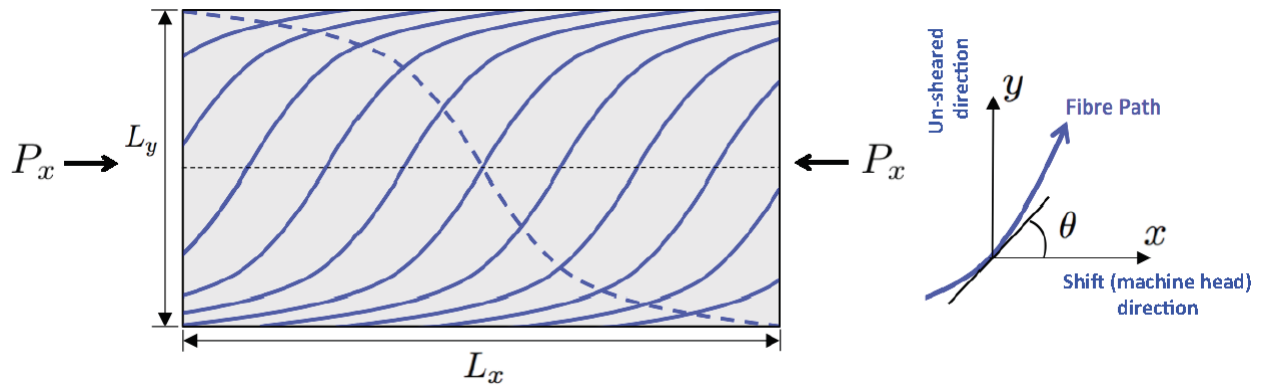


Figure 2: Model setup for panel design problem, showing multiple $+\theta(y)$ fiber paths and a single $-\theta(y)$ path.

from a coupling between fiber angle and thickness, a by-product of the shearing mechanism. As the material shears, total fiber volume is conserved, causing fibers to stack on-top of one another. If t_b defines the un-sheared ply thickness and θ the tow angle relative to the shifting direction (in this note the x - direction) then CTS thickness is

$$t(\theta) = \frac{t_b}{\sin \theta}, \quad (1)$$

as shown in Fig. 1 (right). It should be noted that for CTS the un-sheared orientation is constrained to be perpendicular to the shifting direction.

This technical note reveals the potential weight reductions of composite panels when both buckling and manufacturability constraints are imposed. Considering the buckling of a typical aircraft wing skin, the nonlinear optimisation problem presented shows theoretical designs that offer significant weight savings. For the example considered, optimum CTS designs show 38% weight savings over conventional straight fiber designs, and 34% saving over existing automated fiber placed tow steered technology. The implications of further constraints on panel strength, damage tolerance and manufacturing cost are discussed.

II. Method

The skin panel of length L_x and width L_y is constrained to carry a design load P_x^c which is applied as compressive uniform axial strain (end-shortening) in x , see Fig.2. Longitudinal edges are stress free, whilst (out-of-plane) all edges are simply-supported. In this example the laminate comprises of eight plies with equal base thickness $t_b > 0$ and density ρ , arranged in a fully uncoupled Winckler laminate⁹ $[+\theta, -\theta, -\theta, +\theta, -\theta, +\theta, +\theta, -\theta]$. The fiber angles are assumed prismatic (i.e. $\theta(y)$ is a variable in y but constant in x), symmetric about the mid-width and constrained so that $15^\circ \leq \theta(y) \leq 90^\circ$. These angle constraints imply the fiber path is both anti-symmetric and monotonic, whilst the layer thickness, $t(\theta)$, remains finite (1).

The optimisation problem is to find base thickness t_b and fiber angle $\theta(y)$ which minimises the mass (M) of the CTS, AFP or straight fiber panel subject to a buckling and minimum radius of curvature (R_{\min}) constraint, i.e.

$$\min_{t_b > 0, \theta(y)} M(t_b, \theta(y)) = \rho L_x \int_0^{L_y} \frac{N_{ply} t_b}{\sin \theta(y)} dy \quad \text{such that} \quad \kappa(y) = \frac{d\theta}{dy} \cos \theta \leq R_{\min}^{-1} \quad \text{and} \quad P_x(t, \theta) \geq P_x^c,$$

where ρ is the material density.

To make the optimisation problem amenable to analysis, $\theta(y)$ is restricted to a finite dimensional subspace characterised by a piecewise linear interpolation of discrete values θ_j defined at N equally spaced control points. The location of control points could be introduced as additional design variables. However, for this optimisation problem it is not a good idea, since once control points are free there is no longer a unique mapping between design variables and a global fibre path, resulting in a much more complex optimisation space. In this technical note the constrained, $N + 1$ dimensional, optimisation problem is solved using an interior point algorithm (`fmincon`¹⁰). For the stacking sequence chosen, in and out-of-plane deformations are un-coupled, therefore local laminate stiffness is characterised by in-plane, out-of-plane and through-thickness shear matrices $\mathbf{A}(y)$, $\mathbf{D}(y)$ and $\mathbf{H}(y)$, respectively. To evaluate the buckling load two finite element calculations are carried out. Firstly, the pre-buckled stress field is computed using standard plane stress equations, then the buckling load is evaluated by formulating the linear eigenvalue problem, for which Reissner-Mindlin plate theory is used. For both finite element calculations, the plate is discretised into 1024 rectangular elements, whereby displacements and rotations are interpolated with linear shape functions and the resulting element stiffness matrices are computed using selective Gaussian integration to prevent shear-locking.¹¹ The inclusion of the fiber curvature and plate buckling constraints, as well as the nontrivial coupling between fiber angle and thickness (1) leads to a complex nonlinear optimisation problem. To improve the convergence towards (at least) a *good* local minima, the optimization regime is started with a single control point (i.e. a straight fiber design) $N = 1$ and variable base ply thickness t_b . The optimum design for N control points is then mapped onto fiber angles at $N + 1$ control points using linear interpolation. This provides a starting guess for the subsequent optimisation step. Refinement continues until the mass converges within a prescribed tolerance which, in the results to follow, is taken to be $\pm 0.01\text{kg}$. Within the constraints of this optimisation problem (e.g. monotonicity of the fibre path) tests of the solution procedure and interior point algorithm have shown to provide a robust optimisation strategy leading to repeatable design solutions under changes to the initial design. It is noted that all calculations are carried out within an bespoke in-house MATLAB code.

III. Results

For the results presented here orthotropic ply properties are assumed constant: $E_1 = 130\text{GPa}$, $E_2 = 9.25\text{GPa}$, $\nu_{12} = 0.36$, $G_{12} = G_{13} = 2G_{23} = 5.13\text{GPa}$ and $\rho = 1.584 \times 10^{-6} \text{ kg/mm}^3$. In order to compare the theoretical optimum fibers paths for AFP and CTS manufacturing methods against a straight fiber optimum, a specific panel geometry ($L_x = 750\text{mm}$ by $L_y = 250\text{mm}$) is chosen. Such a choice ensures the minimum radius of curvature constraint ($R_{\min} = 500\text{mm}$ for AFP and $R_{\min} = 30\text{mm}$ for CTS) is active in each case. The panel is subject to a design load of $P_x = 250\text{kN}$ applied as uniform end-shortening.

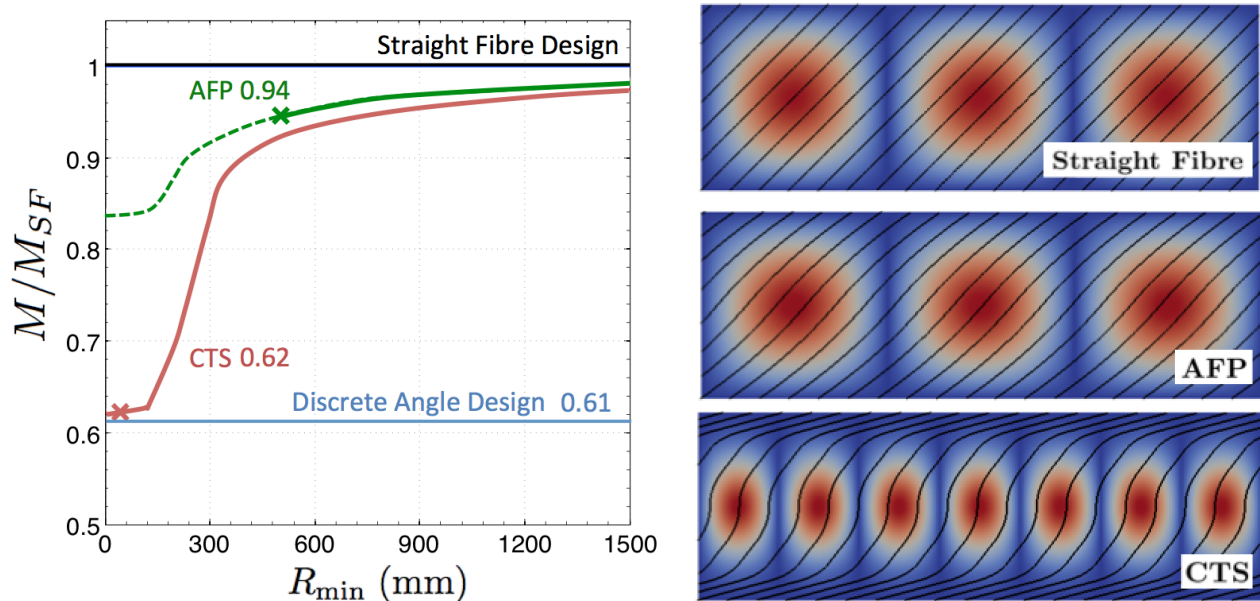


Figure 3: (Left) Panel Masses (normalised against straight fiber mass M_{SF}) versus radius of curvature constraints for optimum AFP and CTS designs. Crosses denote limits of manufacturability. (Right) Mode shapes and fiber paths of minimum mass straight fiber, AFP and CTS (manufacturable) designs.

Figure 3 (left) shows plots of curvature constraint R_{\min} against the optimised panel masses for AFP and CTS normalised relative to the straight fiber optimum. The limits of manufacturable designs are marked (\times). The corresponding optimal fiber paths and buckling modes are shown in Fig. 3 (right), whilst table 1 summarises the key design parameters.

	$M(\text{kg})$	$t_b(\text{mm})$	$\theta_{\min}(\text{°})$	$\theta_{\max}(\text{°})$	$R_{\min}(\text{mm})$	$T_{\min}(\text{mm})$	$T_{\max}(\text{mm})$	N
Straight fiber	1.93	0.82	45	45	∞	6.56	6.56	1
AFP	1.83	0.77	34	50	500	6.16	6.16	7
CTS	1.20	0.27	15	90	30	2.16	8.35	17

Table 1: Summary of key results for optimised Straight fiber, AFP and CTS panels.

Irrespective of the manufacturing constraints, optimal AFP panels are bounded below by all CTS designs. This is attributed to the freedom to tailor local thickness (1) in CTS designs. The thick panel edges

with straight fiber angles ($\theta \sim 15^\circ$) attract compressive load towards the supported panel boundaries, in effect creating an integrated stiffener. Conversely, the unsupported middle of the panel is much thinner, attracting minimal load, yet the shallow angles ($\theta \sim 90^\circ$) locally increases the laminate bending stiffness in the y direction (i.e. increase D_{22}). This significantly increases the overall buckling resistance of the panel, causing the CTS panel to buckle into a higher energy mode compared to the straight fiber design, Fig. 3 (right). If manufacturing constraints are also taken into account the analysis suggests that CTS provides a manufacturable design with a 32% greater weight saving over the AFP optimum. It is interesting to note that little mass saving is achieved once the radius of curvature is less than $\simeq 100\text{mm}$. This implies that the optimal fiber path for buckling has a finite curvature. Extending the analysis for different panel geometries, it is apparent that this critical curvature is dependent on panel width. Actually, the optimum fiber path is independent of panel geometry, apart from the fact that, for narrower panels, angles have to be steered more rapidly from $\theta \simeq 15^\circ$ at the edge to $\theta = 90^\circ$ in the middle.

IV. Discussion & Concluding Remarks

In this study panels have been optimised for minimum mass subject to buckling performance and manufacturing curvature constraints. Various other factors that have not been included in the optimisation problem (e.g. in-plane strength, damage tolerance and speed/cost of manufacture) are now discussed. With only the low fidelity 2D model applied here, assessing the relative strengths of the AFP and CTS designs is difficult. Curving tows using AFP leads to tow gaps and overlaps, whereas CTS fibers paths naturally tessellate, Fig. 1. Intuitively, due to improved part quality, CTS would be expected to outperform AFP. For both AFP and CTS optimal designs steered angles pass through 30° . This causes a local peak in A_{12}/A_{22} (i.e. laminate Poisson's ratio), which may induce in-plane failure as the resin, perpendicular to the fibers, begins to fail in tension. Optimal fiber paths which also comply with strength constraints may be significantly different from those seen in Fig. 3 (right). Furthermore, these designs show that, for maximum buckling resistance, fibers are steered to increase stress in the vicinity of the supports at the panel boundaries. Although this increases stiffness, it makes this region susceptible to critical damage growth from impact or defects. Damage tolerant laminates have been developed with tailored surface layers to protect highly stressed regions¹², and could readily be combined with optimal curved fibers paths found here.

Close to the boundaries, CTS design is reasonably thick (8.35mm) relative to the panel width ($L_y = 250\text{mm}$), which brings into question the accuracy of Reissner-Mindlin plate theory (first order shear theory) for these plate designs. For this thickness to panel width ratio, a one-off calculation shows that there is only a 0.25% difference between buckling loads for first and third-order shear theory.¹³ Since also the optimal design agrees with physical intuition; the results suggest that first order plate theory is sufficient

	$M(\text{kg})$	$\theta_1(^{\circ})$	$\theta_2(^{\circ})$	$t_1(\text{mm})$	$t_2(\text{mm})$	$w_1(\text{mm})$	$w_2(\text{mm})$
Discrete fiber design	1.17	16.2	63.5	0.95	0.27	41.2	83.8

Table 2: Summary of optimal design for a discrete four strip panel. Here w_i denotes the width of the i^{th} strip. We note that only two strips angles are given since the design is symmetric, and strip one is adjacent to the longitudinal boundary.

to obtain representative designs for optimal CTS panels under both bucking and manufacturing constraints, the primary aim of this note. However, it may be an interesting future avenue of research to investigate the sensitivity of the optimal design with respect to different order shear theories.

A key advance of CTS is the ability to steer tows through tight angles without generating defects. As yet, CTS has only been developed for flat structures, but the additional degrees of freedom in the laying head, might allow more flexibility in depositing fibers over complex geometries. Often manufacturing quality is critical in these regions, since any small imperfections can lead to severe manufacturing induced defects such as wrinkles.¹⁴ Whilst CTS may provide significant improvements in product quality, this must be balanced against deposition rate, which when compared to AFP technology is very slow. Investment in addressing these issues is essential for industrial application of this novel technology.

This technical note demonstrates the potential weight savings that are possible, when both angle and thickness are simultaneously tailored. Therefore one possible option, is to lay prismatic strips with constant angles of a given thickness. Solving this optimisation problems for a 4 strip plate, where angles, thickness and strips widths are free, comparable optimum mass designs can be achieved compared to CTS designs, Fig. 1. The optimum designs are summarised in table 2. The main advantage of such designs is that they can be manufactured very quickly, for example using Automated Tap Laying (ATL). However the joints between adjacent strips, in terms of strength will become critical, and how easily such prismatic designs could be used for more complex geometries is an open question.

References

¹Gürdal, Z. and Olmedo, R. ‘Composite Laminates with Spatially Varying Fiber Orientations: Variable Stiffness Panel Concept,’ *AIAA Journal*, Vol. 31, No. 4, April 1993, pp. 751-758. *AIAA J.* **31**, pp. 751-758, 1993.

²Butler, R. and Liu, W., ‘Buckling optimization of variable-angle-tow panels using the infinite-strip method’. *AIAA Journal*, 51 (6), pp. 1442-1449, 2013.

³White, S., Weaver, P. M., and Chauncey Wu, K. ‘Post-buckling analyses of variable-stiffness composite cylinders in axial compression’. *Composite Structures*. 123, pp. 190-203, 2015.

⁴Hyer, M. W., and Charette, R. F., ‘The Use of Curvilinear Fiber Format in Composite Structure Design’, *AIAA Paper* 1989-1404, 1989.

⁵Beakou, A., Cano, M., Le Cam, J. B. and Verney, V., ‘Modelling slit tape buckling during automated prepreg manufacturing: A local approach’, *Compos Struct*, 83, pp. 2628-2635, 2011.

⁶Kim, B. C., Weaver, P. M., Potter, K., 'Manufacturing characteristics of continuous tow shearing method for manufacturing of variable angle to composites' *Composites: Part A* 61, pp 141-151, 2014.

⁷Rhead A. T., Dodwell T. J. and Butler R. 'The effect of tow gaps on compression after impact strength of robotically laminated structures', *CMC: Computers, Materials & Continua*, 35, pp. 1716, 2013.

⁸Kim, B. C., Potter, K. D. and Weaver, P. M. 'Continuous tow shearing for manufacturing variable angle tow composites'. *Composites, Part A: Applied Science and Manufacturing*, 43, pp. 1347-1356, 2012.

⁹Winckler, A. J. 'Hygrothermally curvature stable laminates with tension-torsion coupling', *J. Am. Helicopter Soc.*, 30, pp. 56-58, 1985.

¹⁰Byrd, R. H., Hribar, M. E. , and Nocedal, J., 'An Interior Point Algorithm for Large-Scale Nonlinear Programming', *SIAM Journal on Optimization*, 9, pp.877-900, 1999.

¹¹Hughes, T. J. R., *The Finite Element Method: Linear Static and Dynamic Finite Element*, Dover Publications, New York, 2000.

¹²Butler, R., Rhead, A. T., Liu, W. and Kontis, N. 'Compressive strength of delaminated aerospace composites'. *Philosophical Transactions of the Royal Society A - Mathematical Physical and Engineering Sciences*, 370 (1965), pp. 1759-1779, 2012.

¹³Groh, R. M. J., Weaver, P. M., White, S., Raju, G., Wu, Z. 'A 2D equivalent single-layer formulation for the effect of transverse shear on laminated plates with curvilinear fibres, *Composite Structures*, 100, pp 464-478, 2013.

¹⁴Dodwell, T., Butler, R. and Hunt, G. 'Out-of-plane ply wrinkling defects during consolidation over an external radius'. *Composites Science and Technology*, 105, pp.151-159, 2014.